Constructing soft substrate-less platforms using particle-assembled fluid-fluid interfaces and their prospects in multiphasic applications

Lee, Hiang Kwee; Lee, Yih Hong; Phan-Quang, Gia Chuong; Han, Xuemei; Koh, Charlynn Sher Lin; Ling, Xing Yi

2017

Lee, H. K., Lee, Y. H., Phan-Quang, G. C., Han, X., Koh, C. S. L., & Ling, X. Y. (2017). Constructing soft substrate-less platforms using particle-assembled fluid–fluid interfaces and their prospects in multiphasic applications. Chemistry of Materials, 29(16), 6563-6577. doi:10.1021/acs.chemmater.7b02227

https://hdl.handle.net/10356/143343

https://doi.org/10.1021/acs.chemmater.7b02227

Constructing soft substrate-less platforms using particle-assembled fluid-fluid interfaces and their prospects in multi-phasic applications

Hiang Kwee Lee,[1,2+] Yih Hong Lee,[1+] Gia Chuong Phan-Quang,[1] Xuemei Han,[1] Charlynn Sher Lin Koh,[1] Xing Yi Ling[1]*

[1] Division of Chemistry and Biological Chemistry, School of Physical and Mathematical Sciences, Nanyang Technological University, 21 Nanyang Link, Singapore 637371.

[2] Institute of Materials Research and Engineering, A*STAR (Agency for Science, Technology and Research), 2 Fusonopolis Way, Innovis, #08-03, Singapore 138634.

ABSTRACT: Particle-assembled fluid-fluid interfaces give rise to soft substrate-less platforms with wide-ranging applications, including remote and on-demand manipulation, optical modulation, catalysis, multiphase and multiplex sensing, as well as in-situ reaction kinetics elucidation. Notably, these soft platforms are easy to fabricate and can exhibit long-range order, both of which are challenging to achieve using traditional solid-based substrates. In this perspective, we provide an overview of the latest research in the fabrication and applications of these soft platforms. We begin with a brief discussion on the formation mechanism of two- and three-dimensional substrate-less platforms, followed by highlighting the unique properties of these platforms. We also discuss the application of these particle-assembled interfaces to three specific research areas, including dynamic tuning of optical properties, multiplex molecular sensing, and small-volume reaction modulation and kinetics monitoring. We end our perspective with an outlook on the promising research frontiers that can be achieved using these soft substrate-less platforms.

Introduction

Fluid-fluid interfaces assembled with micro-/nanosized particles are emerging substrate-less platforms that retain a liquid's "soft" and fluidic nature.[1-4] The assembly of these substrate-less ensembles is mainly driven by the reduction of large interfacial tension between immiscible liquid-liquid and liquid-air systems.[5-7] Particles spontaneously adsorb and are trapped at these interfaces to minimize overall Gibbs free energy of the system, even in the absence of external mechanical forces. Generally, particle-fluid platforms can be categorized into two- (2D) or three-dimensional (3D) platforms.[8, 9] These platforms typically require only one fabrication step, and do not require specific and/or complex fabrication techniques commonly employed in substrate-based platforms.[10-13] 2D platforms are formed by assembling particles onto a planar interface between two immiscible fluids using sample volumes in the milliliter to liter range.[14, 15] The platforms are highly scalable, extending up to several tens of centimeters. On the other hand, 3D particle-assembled interfaces usually adopt a spherical structure and are prepared by adsorbing particles onto liquid droplets.[7, 16-18] Furthermore, these droplet-based templates can be easily miniaturized to milli- and micrometric size by using corresponding volumes of liquid droplets during platform fabrication.

Particle-assembled fluid-fluid interfaces exhibit numerous properties, enabling these substrate-less platforms to demonstrate tremendous potential in wide-ranging applications, including remote manipulation, optical modulation, catalysis, and in the broad field of microfluidics. Through a careful selection of particles used during fabrication, these interfacial platforms can be rendered magnetic-, plasmonic-, and catalytic-active.[19-22] Furthermore, these particle-assembled interfaces are ideal for novel multiphasic applications because they have direct access to both the immiscible fluids. These applications include multiplex sensing across fluid-fluid interfaces and tracking of microscale reaction kinetics, rendering such soft interfaces relevant to the broad fields of synthetic chemistry, nanotechnology as well as environmental and industrial safety where processes comprising multiple fluids are prevalent.[23-28] Due to their "softness", particle-assembled fluid-fluid interfaces provide a versatile strategy to produce interfacial platforms with tunable size and shape. For instance, 3D platforms can take on spherical or puddle morphologies which are determined by the interplay between surface tension and gravity. This physical flexibility enables direct control over their mechanical properties such as robustness, specific surface area, and porosity of the assembled particles.[7, 29-31] Moreover, the "malleability" of these soft interfaces enable them to access narrow fluidic channels easily, and allow them to be integrated with state-of-the-art microtechnologies such as lab-on-a-chip devices.[32-36] Integrating interfacial particle assemblies with microdevices is important especially with growing efforts to down-scale bio(chemical) processes for high throughput screening and environmental conservation through minimal chemical consumptions.[37-40]

Another vital attribute of particle-assembled fluid-fluid interface is its ability to achieve novel long-range crystallinity with uniform orientation in both 2D and 3D that is challenging to attain using other fabrication methods.[22, 41, 42] Such unique advantage of interfacial particle assembly is due to the highly mobility of particles at fluid-fluid interface where individual building blocks can continuously organize and orient to achieve a minimum global free energy.[43-45] Long-range order is crucial to impart distinct collective effects arising from the

crystalline structure which are not observed in individual particles. Consequently, particle-assembled fluid-fluid interfaces hold tremendous promise in realizing an extensive library of distinct structure-to-function phenomena. These collective benefits therefore motivate us to summarize current research status of soft particle-assembled interfaces to highlight major achievements and identify scientific gaps that could further expedite interfacial platforms towards real-life applications.

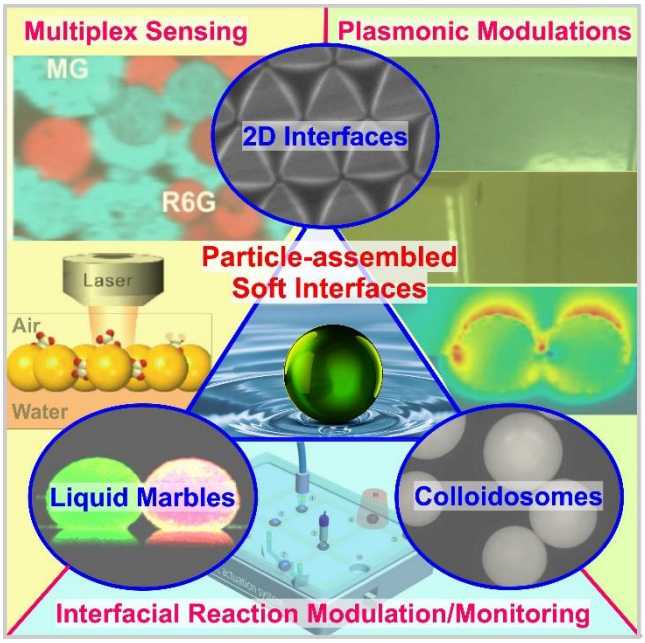

Figure 1. Overview on the various types of particle-assembled fluid-fluid interfaces and their interfacial applications. Reprinted with permission from ref 33, 29. Copyright 2014, 2015 Wiley-VCH verlag GmbH & Co. Reprinted with permission from ref 22. Copyright 2015 Nature Publishing Group. Reprinted with permission from ref 98, 77. Copyright 2013, 2016 Royal Society of Chemistry. Reprinted with permission from ref 51, 28. Copyright 2013, 2016 American Chemical Society.

In this perspective, we review the latest progress in the development of particle-assembled fluid-fluid interfaces as substrate-less platforms and their interfacial applications (Figure 1). Our perspective is in no way comprehensive, and readers are encouraged to refer to other outstanding reviews for details on the formation mechanism and molecular-assembled interfaces.[14, 15, 46-49] We begin by describing various particle-assembled platforms formed on macroscopic 2D fluid-fluid interfaces, followed by the shrinking of these soft interfaces into 3D spherical templates comprising millimeter-sized liquid marbles and microscopic colloidosomes. Emphasis will be placed on their fabrication, as well as their unique physical/mechanical characteristics which can be leveraged upon to achieve additional advantages over traditional substrate-supported particle platforms. Subsequently, we discuss the applications of these soft particle-fluid platforms on three main areas: (1) dynamic modulation of particle-induced plasmonic properties, (2) multiplex molecular detection, and (3) small-volume reaction modulation and monitoring. Finally, we will conclude our discussion and present an outlook on possible avenues for exploration to further expand particle-assembled soft interfaces as fluid-based metamaterials and smart devices for next-generation sensing, catalysis, artificial biomimetics, and light-matter interactions.

1. Types of particle-assembled fluid-fluid interfaces

1.1 Two-dimensional (2D) particle assembly at soft fluid-fluid interface

Bulk fluid-fluid interfaces are appealing platforms to organize nanoparticles into superlattices with excellent long-range order.[14, 15] Micro-/nanosized particles adsorb spontaneously at the interface to minimize interfacial free energy, allowing monolayers of nanoparticles to be easily trapped and assembled at these interfaces. These particles also retain excellent lateral mobility at the interface, thereby creating an ideal platform for the scalable organization of nanoparticles.

To assemble particles at the liquid-gas interface, a relatively non-polar colloidal particle dispersion phase is typically spread over an underlying immiscible polar subphase.[50] The liquid subphase usually has a high surface tension such that the interfacial trapping energy dominates gravity, resulting in a skin effect to prevent the submersion of particles into the subphase. Consequently, solvents such as water and diethylene glycol are frequently employed as the subphase due to their extensive network of intermolecular hydrogen bonds, which effectively traps particles at the soft interface to form a Langmuir film. A systematic surface compression can also be introduced to modulate the particle packing density within the Langmuir film, enabling the creation of a sparsely packed monolayer to a compact one where adjacent particles are directly contacting each other (Figure 2A).[51] This modulation is analogous to the continuous transition of the Langmuir film from a 2D "gas" to "liquid", and eventually to a "solid" film (Figure 2B); these monolayers can be subsequently transferred onto solid substrates via either Langmuir-Blodgett or Langmuir-Schaefer techniques. Using Ag nanocube monolayers as an example, increasing surface pressure brings the nanocubes in the monolayer closer to each other (Figure 2B). This decrease in interparticle separation causes the monolayer film color to transition from yellow green (Π = 8 mNm^{-1}) to brownish yellow (Π = 10 mNm^{-1}), and eventually to metallic silver (Π = 18 mNm^{-1}).[51]

A rich library of superlattices has been demonstrated using this assembly approach, including various close-packed assemblies using Platonic nanoparticles, [52, 53] prisms, [54] nanorod,[55, 56] and wires[35] as building blocks, as well as binary/ternary nanocrystal superlattices. [57-60] In the self-assembly of shape-controlled nanoparticles at the liquid-air interface, shape entropy has also brought about superlattice structural diversity of various upconversion nanoplates[61] (Figure 2C) and bipyramids/bifrustums (Figure 2D).[41] Despite the vast potential afforded by the liquid-air platform, a significant shortcoming of this approach lies in its inherent requirement of spreading relatively hydrophobic particles in conjunction with a polar liquid subphase. However, recent advances have begun utilizing electrospraying to introduce aerosolized particles dispersed in polar solvents at the liquid-air interface during the self-assembly process with considerable success.[62] We can therefore expect even more widespread adoption of the liquid-air interface to organize particles with various surface functionalities in the future.

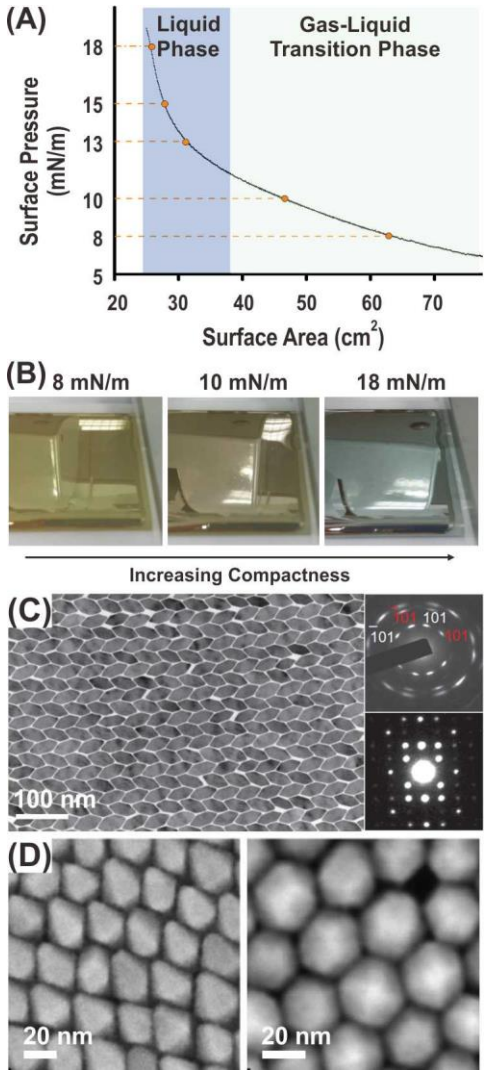

Figure 2. (A) Isotherm and (B) photographic images of the Langmuir films when mechanically compressed to various surface pressures. Reprinted with permission from ref 51. Copyright 2013 American Chemical Society. (C) 2D superlattices of upconversion nanoplates. Reprinted with permission from ref 61. Copyright 2013 Nature Publishing Group. (D) Self-assembly of bipyramids (left) and bifrustums (right). Reprinted with permission from ref 41. Copyright 2014 American Chemical Society.

In addition to the liquid-air interface, the liquid-liquid interface is another widely utilized platform to organize nanoparticles into ordered structures. Typically comprising a polar aqueous phase and a non-polar organic phase, an interfacial potential well is created between these two immiscible liquids which can effectively trap nanoparticles at the liquid-liquid interface.[1, 14, 63] Such trapping occurs regardless of the nature of the particle surface chemistry and the dispersion solvent, thereby overcoming the intrinsic experimental limitations at the liquid-air interface. In addition to the abovementioned factors used to tune particle assembly at liquid-air interfaces, liquid-liquid interfacial systems also offer additional parameters such as buoyancy and two concurrent particle-liquid interactions (particle-aqueous and particle-organic) to systematically modulate the interfacial behaviors of the particles. This assembly approach has been successfully adopted together with electrostatic interactions to assemble non-close-packed hexagonal arrays of polystyrene particles, with interparticle spacing ranging 3 to 10 particle diameters.[64] Such regular and sparsely-positioned array can be crucial for biosensing to minimize cross-talk between various sample points. Electrostatic interactions have further been utilized in conjunction with supramolecular polymer filament templates to guide the self-assembly of Au nanoparticles into plasmonic waveguides.[65] Moreover, hierarchical structures can also be achieved at liquid-liquid interfaces via breath figures-based self-assembly, in which hexagonal arrays of micro-sized water droplets are introduced to the surface of a polymer solution.[66, 67]

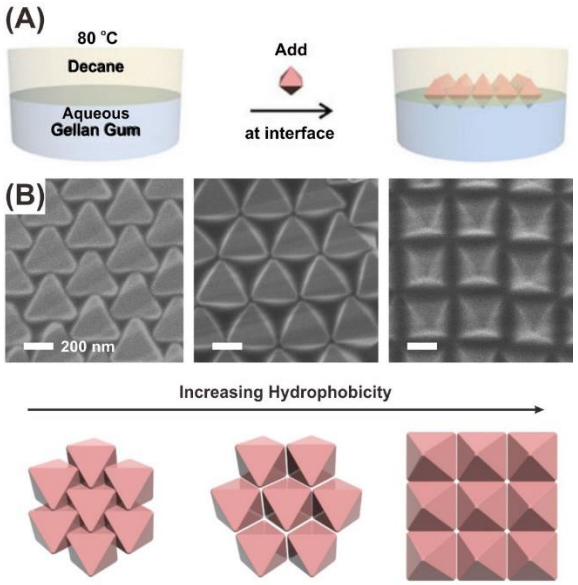

Figure 3. (A) Schematic representation on the self-assembly of Ag octahedra on the liquid-liquid interface created between immiscible decane and aqueous solution of gellan gum. (B) Using liquid-liquid interface to tune plasmonic metacrystal structure of Ag octahedra by modifying the particle surface hydrophobicity. Reprinted with permission from ref 22. Copyright 2015 Nature Publishing Group.

Our group has also established the concept of "one nanoparticle, multiple superlattices" at the water-oil interface to achieve superlattice structural diversity without changing nanoparticle morphology (Figure 3A).[22, 42] By tailoring the nanoscale surface chemistry of shape-controlled nanoparticles such as nanocubes and octahedra, we demonstrate that each particle morphology can be individually assembled into three distinct superlattices at the water-oil interface. Using Ag octahedra as an example, we systematically increase the surface hydrophobicity of the nanoparticles, which leads to a continuous evolution of superlattice structure from hexagonal close-packed arrays to progressively open square lattices with particles standing on their vertices (Figure 3B). As the superlattices evolve, the building blocks change from a planar to a vertical configuration with increasing contact with the oil phase. Such interfacial behavior variations arise from increasingly favorable particle-organic phase interactions between the hydrophobic alkylthiols and the organic phase. We further demonstrate the importance of superlattice design for sensing by elucidating the creation of plasmonic "hotstrips" in the square lattice, leading to ~130-fold boost in local electromagnetic field enhancement.

While the significance of bulk interfaces in directing 2D particle assembly is clearly exemplified, the soft platforms generated are usually microscopically flat and prepared using substantial sample amounts (in the milliliters to liters range).

As such, the platforms are susceptible to laser misalignment in spectroscopic applications and face limitations for miniaturized applications. This raises the scientific question of "Are we able to break the planar geometry to achieve functional miniature 3D soft interfaces?" Due to their enhanced surface areas and increased tolerance to optical misalignments during spectroscopic studies, we hypothesize that micro-/nanoscale 3D soft interfaces can facilitate future integration into microdevices and technologies, and at the same time offer an artificial microenvironment to mimic/study cellular systems.

1.2 Miniature 3D particle-assembled fluid-fluid interface

1.2.1 Liquid Marbles

Liquid marbles are macroscopic 3D particle-encapsulated liquid droplets with diameters in the millimeter to centimeter range.[3, 18] The formation of liquid marble mainly utilizes high-surface tension water microdroplet, but can also be extended to other organic liquids such as toluene and chloroform.[68] As with bulk interfaces, particles also spontaneously cluster onto such 3D liquid-air interfaces to minimize the system's free energy. This fabrication approach effectively isolates the microdroplet within a loosely packed particle shell, thus significantly reducing the rapid evaporation rates typical in small-volume liquids.[69] For instance, graphene liquid marbles decrease the evaporation of the enclosed droplet by two-fold as compared to an exposed droplet.[70] However, the use of pulverized particle powders for liquid marble formation also implies that liquid marbles predominantly do not possess crystalline assembled structures at these 3D liquid-air interfaces. Nevertheless, the presence of air pockets between adjacent particles on the enclosed liquid droplet surface confers Cassie-Baxter-type anti-wetting properties to minimize particle-water contact, analogous to the superhydrophobic "lotus effect".[24] Consequently, liquid marbles are non-stick and can be easily manipulated on both solid and liquid surfaces without leakage, even on hydrophilic surfaces (Figure 4A).

Liquid marbles possess excellent mechanical robustness, and are capable of bouncing at elevated heights. They can also merge or split on demand without disintegrating due to the particle shell's self-healing property; minimization of interfacial free energy implies that the newly split marbles will also be fully encapsulated with particles. (Figure 4B).[7, 24, 71] This robustness of liquid marbles during merging offers an appealing alternative to homogenize the contents of multiple microdroplets for the initiation of chemical reactions without requiring engineered microfluidic systems.[71] In addition, liquid marbles prepared using hydrophobic particles can also be stably suspended atop water to create water-particle-water interfaces.[72] Such configuration enhances droplet stability against evaporation by four-fold as compared to liquid marbles in the air-particle-water configuration, due to increased humidity around the liquid marbles.[73] This stability will be crucial in applications which require extended tracking of time-based events, such as in reaction kinetics monitoring. Aside from suspending atop water, liquid marbles can also be submerged within organic liquids to form oil-particle-water interfaces (Figure 4C).[24, 74] This direct contact of liquid marbles with an external liquid phase therefore extends their soft interfaces into a variety of fluid-fluid configurations, and will enable liquid marbles to be utilized in diverse interfacial studies and applications, which target potential gas- and/or liquid-related processes at fluid-fluid interfaces. One possible example of these processes involves gas scrubbing by liquid absorbents, whereby gas molecules dissolve in liquid absorbent upon their physical contact.

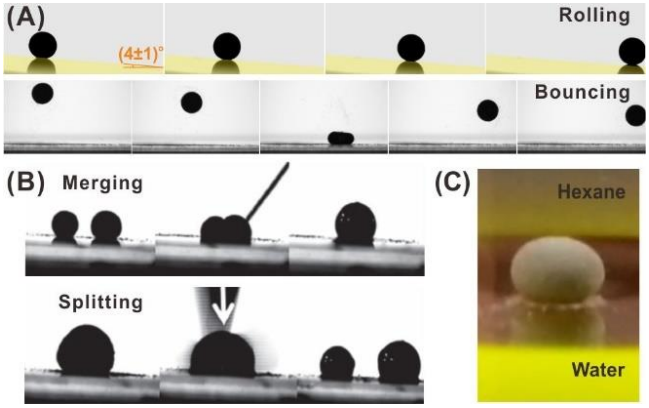

Figure 4. (A, B) Digital images of liquid marble rolling, bouncing, merging and splitting. Reprinted with permission from ref 24. Copyright 2014 Wiley-VCH verlag GmbH & Co. Reprinted with permission from ref 71. Copyright 2012 Wiley-VCH verlag GmbH & Co. (C) Submersion and floating of a plasmonic liquid marble in hexane and on water (yellow layer), respectively. Reprinted with permission from ref 24. Copyright 2014 Wiley-VCH verlag GmbH & Co.

The most outstanding feature of liquid marbles lies in the facile integration of additional functionalities by changing the types of encapsulating materials. This feature implies that liquid marbles are analogous to a painter's blank canvas, wherein the potential properties achievable using liquid marbles are only limited by one's imagination. As an example, liquid marbles prepared using plasmonic-active Ag nanocube generates intense electromagnetic fields across the entire 3D shell.[24] These enhanced electromagnetic fields boost surface-enhanced Raman scattering (SERS) signals by > 10^8-fold, enabling ultrasensitive read-out of molecular vibrational signatures. Likewise, catalytically-active liquid marbles can also be prepared by assembling noble metal particles (Ag or Au) on the surface of an aqueous methylene blue microdroplet.[75] The metallic shell acts as an electron relay to improve the catalytic degradation of this environmental toxin. This "reaction core-catalytic shell" configuration is a novel strategy for support-free heterogeneous catalysis, and contrasts with existing methods which mainly immobilize catalytic materials onto secondary solid supports for catalysis.

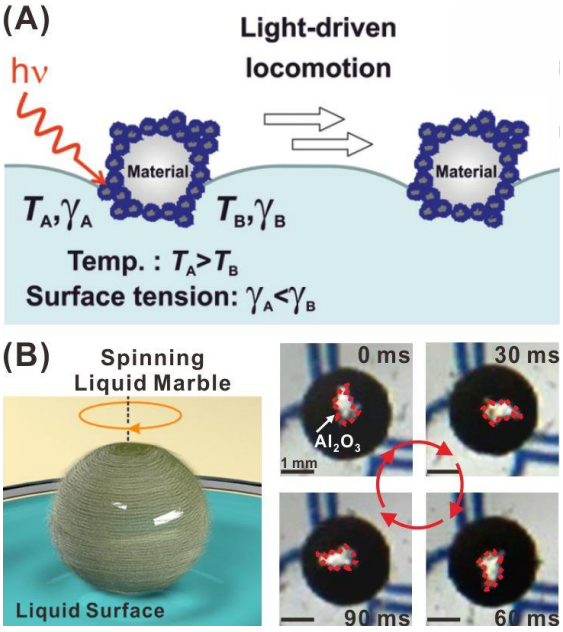

Figure 5. (A) Illustration on the Marangoni-type maneuver of liquid marble when the laser is irradiated on a single face of photothermal-active liquid marble. Reprinted with permission from ref 76. Copyright 2016 Wiley-VCH verlag GmbH & Co. (B) Schematic (left) and actual digital camera snapshots (right) demonstrating the spinning of magnetically-active liquid marble when placed on water surface. The external rotating magnetic field is conveyed using a commercial stirrer and set at 500 rpm. Reprinted with permission from ref 72. Copyright 2016 American Chemical Society.

More importantly, liquid marbles also double as smart microdevices capable of on-demand manipulation and maneuvering. This is achieved by incorporating an active encapsulating shell that is responsive to external stimuli such as photo-irradiation,[76] electric field[18, 77] and magnetic field.[78] Photothermal-active liquid marbles constructed using light-absorbing materials such as polypyrrole, carbon black, and graphene can achieve surface temperatures > 100ºC at the liquid marble shell upon laser irradiation (Figure 5A).[79] When suspended on a water surface, light irradiation creates an asymmetric heat distribution on the liquid marbles, resulting in a surface tension gradient between the bulk water body and the liquid marble surface. This phenomenon in turn enables a Marangoni-type maneuver for the liquid marbles over the water surface, which is then used to control the movement of an external object on water surface. In addition, non-uniform local surface tension created using the evaporation of alcohol encapsulated within liquid marbles followed by their subsequent condensation on the external water surface can also drive liquid marble propulsion.[80] Furthermore, electric-responsive liquid marbles coated with polytetrafluoroethylene (PTFE) particles can be electrically charged by applying an electric field to induce electro-coalescence of adjacent liquid marbles for effective merging of their encapsulated contents.[77]

Among various stimuli-responsive liquid marbles, magnetic-field responsive liquid marbles represent a class of liquid marbles that is extensively investigated because they offer a simple-yet-powerful approach for precise and rapid microdroplet manipulation using an external magnet. These magnetic liquid marbles are typically fabricated using Fe_3O_4 nanoparticles, and the magnetically-responsive shell can also be opened or closed by simply adjusting the distance between the magnet and liquid marble.[33] Additionally, these magnetic liquid marbles (~1 mm diameter) exhibit on-demand and instantaneous movement on both flat and curved solid substrates that are easily controlled using a magnet, achieving a remarkable velocity as high as 0.32 $m.s^{-1}$.[78] The maximum velocity of the liquid marbles is primarily affected by their droplet volumes as well as the magnetic field strengths of both the external magnet and the encapsulating nanoparticles. However, traditional magnetic actuations of liquid marbles are limited to linear motion that only allow simple spatial maneuver of the microdroplets. More recently, our group overcomes this limitation and demonstrates a dynamic spinning of Fe_3O_4-based magnetic liquid marble atop an external water surface, achieving spin rates up to 1300 rpm which are synchronous with the externally applied rotating magnetic field (Figure 5B).[72] The spinning liquid marble introduces a circular hydrodynamic flow and an outward centrifugal force of $\geq 2g$ within the rotating microdroplet which is sufficient to precipitate an aqueous suspension of nanoparticles (~ 100 nm) onto the liquid marble's shell.[81] Both the circular hydrodynamic flow and centrifugal force are essential to accelerate the homogenization of particles/molecules within the encapsulated 3D liquid droplet, thus allowing precise control over the kinetics of chemical processes occurring in the microdroplet.

Given the abundance of functional solids available for microdroplet encapsulation and its ability to form Janus or even more sophisticated multilayered shell,[82] liquid marbles is a truly versatile interfacial-based soft micro-platform suitable for diverse applications. Nevertheless, we note that liquid marble has a macroscopic size with diameter of at least 1 mm. This size restriction potentially impedes their integration into microfluidic channels (typically < 500 µm) of miniature devices like lab-on-a-chip system. The down-scaling of particle-assembled droplets is therefore vital to promote their integration into state-of-the-art microtechnology for high throughput processing and reducing chemical/energy/solvent consumption. We also anticipate the miniaturization of particle-assembled droplets to further boost their specific surface area, which is especially relevant for surface-dependent processes such as heterogeneous catalysis and surface-sensitive molecular detection.

1.2.2 Colloidosomes

Colloidosomes are micrometer-sized particle-stabilized Pickering emulsions constructed using immiscible liquid-liquid interfaces which are > 1000-fold smaller than liquid marbles, with sizes between ~ 1 to 200 µm.[4] They appear as "dust-like" structures and are often described as miniaturized liquid marbles (Figure 6A).[20] Colloidosomes are generated by emulsifying a solution system comprising three different components: the inner encapsulated liquid phase (dispersed phase), the outer liquid phase (continuous phase), and solid particles which can be dispersed in either liquid phase.[83] Colloidosome formation generally requires two steps, involving the initial generation of picoliter droplets and subsequent particle assembly at the liquid-liquid interface. Picoliter droplets can be created by breaking up a relatively large volume of dispersed phase (µL – mL) using microfluidic techniques or physical agitation using stirrers, sonicators and manual emulsification.[29, 83] Colloidal particles then rapidly adsorb at these immiscible microscale interfaces to mitigate their large interfacial energy.[31] Similar to liquid marbles, colloidosomes

can also be imparted with additional properties (catalytic, plasmonic and so on) using various types of functional particles (Figure 6B).[29, 84-87]

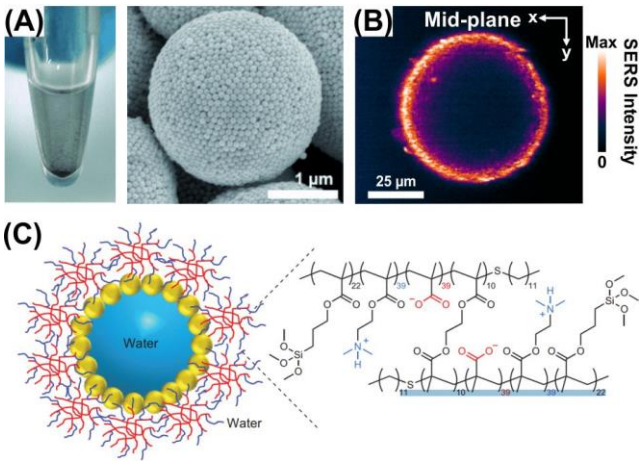

Figure 6. (A) Photo of as-prepared colloidosomes which settled on the bottom of tubes (left) as "dust-like" entities. SEM image (right) of plasmonic colloidosomes formed via self-assembly of Au nanoparticles onto the liquid-liquid interface. Reprinted with permission from ref 20. Copyright 2015 Wiley-VCH verlag GmbH & Co. (B) X-y SERS image recorded from the mid-plane of colloidosome prepared using plasmonic-active Ag nanoparticles. Reprinted with permission from ref 29. Copyright 2015 Wiley-VCH verlag GmbH & Co. (C) Scheme depicting the design and construction of functionalized colloidosomes prepared by TMOS-induced crosslinking and covalent grafting of a novel branched copolymer ($TMSPMA_{23}/DMAEMA_{40}/MAA_{37}$–$EGDMA_8$–$DDT_{10}$) corona on the semipermeable exterior of a close-packed silica nanoparticle shell. pH changes lead to the regulation of net charge associated with cationic dimethylamino (blue) and anionic carboxylate (red) groups of the surface copolymer. This creates a gated response to the transfer of charged small molecules across the inorganic membrane. Reprinted with permission from ref 91. Copyright 2013 Nature Publishing Group.

A distinct advantage of colloidosomes over liquid marbles lies in their ability to control the arrangement of individual building blocks at the microscale liquid-liquid interface. Control over colloidosome shell structure is important in the transformation of colloidosomes into potential soft and ultrasmall metamaterials on a 3D picoliter droplet. The ability to engineer particle organization on the colloidosome shell has a direct impact on its physical properties such as elasticity and porosity of the colloidosomes,[30] which is particularly useful in facilitating interfacial interactions between molecules in phase-separated fluids. Using colloidal particle dispersion during colloidosome formation allows control over particle organization, and contrasts with the use of pulverized particle aggregates for the preparation of liquid marbles. In fact, particle stability in either the continuous or dispersed phase is the main factor governing the physical organization of particles at the colloidosome's liquid-liquid interface.[30] For instance, a monolayer of particle-assembled colloidosome can be achieved if the particles remain well-dispersed in the continuous phase during manual emulsification. On the contrary, a disordered and multilayered particle shell at the soft interface arises from using a continuous phase containing aggregated particles because particle rearrangement at the microscale interface is hindered. A colloidosome shell possessing a low degree of crystallinity can also be constructed using particles that are aggregated in the dispersed phase but are well-dispersed in the continuous phase. The low dispersibility of particles in the dispersed phase reduces particle mobility at the interface, and thus leads to low crystallinity on the colloidosome shell.

Moreover, reinforcement to the colloidosome shell can also be supplemented via post-emulsification treatment to confer additional mechanical robustness required for practical applications. Examples of reinforcement methods include using adhesive polymers[30] or click-chemistry[88, 89] to introduce an additional level of inter-particle connections on top of common non-covalent interactions (electrostatic and van der Waals force). These shell modifications further overcome the fast evaporation of ultrasmall-volume dispersed phase and prevent mechanical disruption to the particle assembly.

The microscale dimensions of colloidosomes bring about two important attributes unachievable in liquid marbles. First, colloidosomes have ultrasmall volumes in the pico/femto-liter range, and this leads to potential > 10^6-fold faster molecular diffusion from the center of the encapsulated droplet to the colloidosome shell as compared to liquid marbles.[90] Colloidosomes therefore do not require external agitation or complex microfluidic design to achieve droplet merging and homogenization. The second attribute of colloidosomes arises from the > 10^3-fold enhancement in specific surface area as compared to those of liquid marbles.[23] The resulting large interfacial area-to-volume ratio aids the swift transfer of mass across the 3D fluid-fluid boundary, which is especially crucial for biphasic applications such as the extraction of target molecules from one solvent to another.

Furthermore, colloidosomes have similar dimensions to many primitive biological structures, enabling them to serve as an ideal artificial platform for biochemical studies. For instance, water-dispersible colloidosomes constructed using silica nanoparticles and pH-responsive surface copolymer are used to mimic the electrostatically gated membrane permeability of primitive cell-like structures (Figure 6C).[91] Selective release and uptake of small molecules are achieved using such artificial protocells. This behavior is important to trigger enzymatic dephosphorylation reactions specifically within the aqueous interior of the artificial chemical cells.

With its distinct advantages, it is therefore unsurprising that colloidosomes are fast evolving as model substrate-less platforms for enhancing interfacial processes, as well as replicating nature-inspired cellular operations for mechanistic and application-oriented studies. With the continuous miniaturization of particle-assembled soft interfaces, we raise the scientific questions of "How much further can we push the minimum size limit of these substrate-less platforms?" and "What additional properties can we garner from such ultrasmall particle-assembled soft interfaces?" Achieving these goals are non-trivial, and will require efficient integration of (sub)nanoscopic particles with size < 10 nm such as quantum/carbon dots and metal nanoclusters with even smaller liquid droplets (diameter between nm to μm) prepared using micro-/nanofluidics.

2. Applications using particle-assembled soft interfaces

Thus far, we have showcased a variety of particle-assembled fluid-fluid interfaces, ranging from 2D platforms to 3D droplet-based template with sizes tunable from the centi-

meter-scale down to the microscale. These structurally diverse superlattices at various interfaces has certainly led to potential applications in wide-ranging fields, including nano-optics,[46, 92] sensing,[1, 93-95] catalysis,[96] and magnetism.[57] However, majority of these applications are demonstrated after transferring the assembled superlattices to a solid platform, and are therefore beyond the focus of our current perspective on the potential applications of substrate-less platforms. Our aim here is to focus on the recent advances in applications based on soft particle-assembled substrate-less platforms rather than to provide a comprehensive review.

2.1 Plasmonic modulations

Substrate-less plasmonic platforms assembled using noble metal (Au, Ag) nanoparticles have received the most scientific attention among the various classes of nanomaterials, with applications demonstrated in optics, analyte detection, photothermal heating,[70, 97] and in-situ spectroscopic monitoring of reaction kinetics. This multitude of applications based on soft plasmonic platforms likely arises from the ease of tailoring the surface chemistry of plasmonic nanoparticles, which in turn enables the creation of structurally diverse superlattices at the interface. More importantly, the associated localized surface plasmon resonances (LSPR) of plasmonic nanoparticles are highly sensitive to changes in their immediate environments. Numerical simulations employed to understand the LSPR of coupled nanoparticles at the water-oil interface shows that the spectral position and relative strength of the plasmon resonance depends on the exact interfacial position of the nanoparticles at the interface.[98] Notably, a near-field coupled mode appears for a dimer at the water-oil interface, which can potentially generate SERS enhancement factors on the order of 10^7 - 10^9 (Figure 7A).

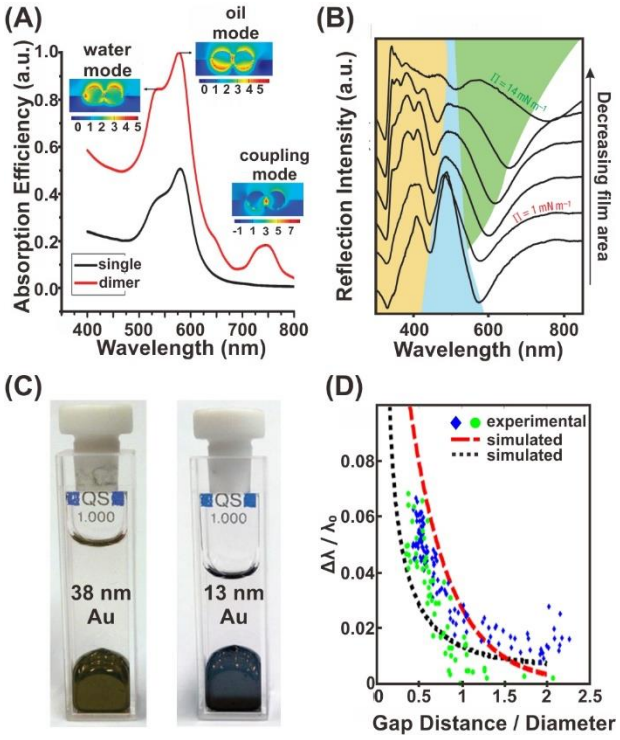

Figure 7. (A) Using 3D-FDTD to simulate the electromagnetic behaviors of Au nanoparticle dimer at the oil/water interface. Reprinted with permission from ref 98. Copyright 2013 Royal Society of Chemistry. (B) Surface pressure-dependent spectral evolution of Ag cuboctahedra monolayer at the air-water interface. Reprinted with permission from ref 99. Copyright 2007 Nature Publishing Group. (C) Monolayers of Au nanoparticles serving as liquid mirror (left) and optical filter (right). Reprinted with permission from ref 101. Copyright 2016 Royal Society of Chemistry. (D) Plasmon ruler demonstrated at the oil-water interface. Blue and green points correspond to experimentally obtained measurements. Black and red dashed lines correspond to theoretically-derived trends using mean-field theory and coupled-dipole approximation respectively. Reprinted with permission from ref 104. Copyright 2012 American Chemical Society.

Modulating particle density and interparticle separation of Ag nanocrystal monolayer at the air/water interface leads to a continuous spectral evolution in the monolayer's optical response across the entire visible spectrum (Figure 7B).[99] At sufficiently high packing densities, metal nanoparticles at the interface lose their colorful hues to form liquid mirror-like films. Liquid Ag mirrors are highly reflective with average reflectance of 77 % in the 400 – 1000 nm range, and is comparable with that of Hg-based liquid mirrors. [100] However, such liquid mirrors are only possible using large nanoparticles. Particle size plays an important role in the optical behaviors of the films formed at the air-liquid interface.[101] Larger Au nanoparticles with 38 nm diameters are well-suited for mirror-based applications, whereas films formed with smaller 12-nm Au nanoparticles with strong absorbance in the green and red regions are more appropriate as optical band-pass filters (Figure 7C). In addition to changes in optical properties, electrical conductivity of metallic films also increases with increasing particle coverages, transitioning from insulating to conducting behaviors.[102, 103]

Plasmon coupling between neighboring nanoparticles gives rise to predictable shifts in the coupled LSPR, and such spectral shifts can be used as a spectroscopic ruler to measure the nanoscale interparticle spacing between the nanoparticles.[104] This spectroscopic ruler, also known as plasmonic ruler, has been established at the liquid/liquid interface using 16-nm Au nanoparticles adsorbed at the water/dichloroethane interface. By controlling the average interparticle spacing between 6 – 35 nm, the in-situ plasmon resonance transmission of the adsorbed nanoparticles can be predictably tuned in accordance to the empirical plasmon ruler equation (Figure 7D).

Despite the multiple benefits enabled by planar soft interfaces, it is also of paramount importance to overcome their inevitable susceptibility to spatial fluctuations caused by thermal/physical agitation. These agitations can arise from the surrounding environment, such as wind, natural ground vibrations and temperature changes. A robust platform is essential for its subsequent incorporation into various devices for practical applications.

2.2 Multiplex molecular sensings

Fluid-fluid interface offers immense opportunities for in-situ multiplex analyte detection, because the incorporation of an additional fluid phase enables simultaneous detection of compounds dissolved in both aqueous and organic phases.[23, 24, 84] Furthermore, this one-step multiplex detection scheme eliminates the need for phase separation processes prior to sample analysis, which are common protocols in analyzing multiphasic samples using gas- or high-performance liquid chromatography. In contrast, in-situ biphasic detection continues to pose significant challenges for conventional sensing using solid substrates and colloidal dispersions. Detection at fluid-fluid interface therefore allows rapid analyses for multiphasic

samples which are ubiquitous in environmental pollution and food safety. Here, we discuss the achievements in fluid-fluid interfacial sensing ranging from non-molecular-specific colorimetric and fluorescence techniques, and eventually to biphasic molecular identification and quantification at the molecular level using SERS.

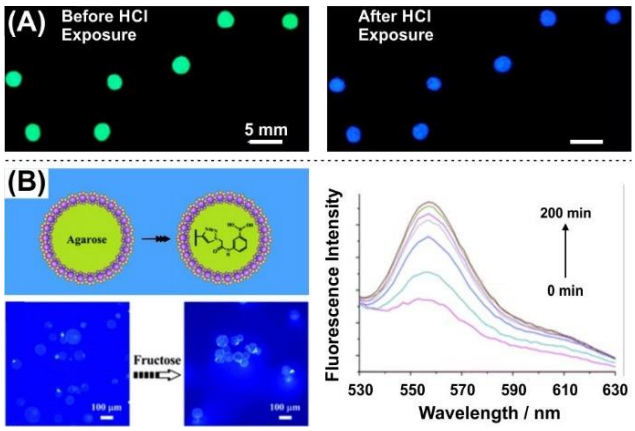

Figure 8. (A) Liquid marbles for gas sensing containing HPTS indicator under UV irradiation (i) before and (ii) after exposure to HCl vapor. Reprinted with permission from ref 105. Copyright 2010 Royal Society of Chemistry. (B) Molecular recognition of fructose with fluorogenic boronic acid embedded on colloidosomes (left). An increase in fluorescence intensity (right) with time was observed upon exposure to fructose. Reprinted with permission from ref 107. Copyright 2013 Royal Society of Chemistry.

Colorimetric sensing is commonly employed to provide a preliminary binary "yes/no" response to detect the presence/absence of target chemical species. The presence of target analytes triggers drastic color changes from an initial dye-based indicator solution. Liquid marbles are often employed for colorimetric detection because they can efficiently encapsulate millimeter-sized indicator microdroplets within a chemical-resistant and porous particle shell. These advantages allow high throughput analyte detection with visually detectable color changes from the microdroplets. For instance, acidic/basic gas detection can be achieved by encapsulating aqueous pH indicator microdroplets within chemical-resistant Teflon powder shell (Figure 8A).[105] Porous liquid marbles containing phenolphthalein changes from colorless to pink upon exposure to basic ammonia vapor, whereas liquid marbles containing trisulfonic acid-based functionalities (HPTS, pKa ~ 7.3) exhibit pH-dependent fluorescent color change from blue (405 nm) at pH 6 to green (450 nm) at pH 8. In addition, colorimetric detection of pH changes can be visualized by the release of an aqueous dye droplet from the rupturing of a pH-responsive liquid marble fabricated using amine-terminated polystyrene beads (PDEA-PS; pKa = 7.3). The presence of an acidic environment rapidly protonates the amine moieties to form hydrophilic cationic-terminated latex particles which causes the liquid marble to rupture within 1 min. These findings establish the use of liquid marbles as proof-of-concept platforms to simultaneously detect analytes in different biphasic environments via a combination of multiple detection mechanisms (e.g. colorimetry and change in fluorescent color). Even though colorimetric sensing offers rapid preliminary results without the aid of sophisticated equipment, there is limited molecular-specific and quantitative information provided.

To address the drawback of colorimetric sensing, common analytical tools such as electrochemical analysis and fluorescence spectroscopy are integrated with particle-assembled soft interfaces to deliver richer information regarding the nature of analytes at the fluid-fluid interface. Interfacial voltammetry has been utilized to quantitatively detect the anticancer drug topotecan across a bulk polarized particle-assembled water/1,2-dichloroethane interface.[106] Identification and quantification of topotecan is based on the energy and current intensity of electrochemical responses associated with the direct molecular transfer of topotecan at the liquid-liquid boundary. Such method enables detection limits of 0.1 μM, with up to 100-fold enhanced selectivity over other anticancer drug molecules and interfering reagents. Fluorescence microscopy has also been used as a turn-on sensor in the use of colloidosomes for fructose detection (Figure 8B).[107] Colloidosomes are grafted with boronic acid-based fructose recognition fluorescent functionalities. The presence of fructose leads to a reversible boronate ester bond formation, which gradually turn "on" the fluorescence emission which increases in intensity with reaction progress. Fructose contents are quantified by the gain in fluorescence intensity. Although these schemes represent facile strategies for sensitive and quantitative detection, the choices of suitable analytes are narrow due to the prerequisite of specific molecular recognition for the system to work. Furthermore, fluorescence peaks have broad full-widths at half maximum in the range of several tens of nanometers, making it difficult to resolve close or overlapping emission peaks in the presence of multiple fluorescent molecules.

The integration of SERS detection with various substrateless plasmonic platforms has significantly advanced the interfacial sensing capabilities of fluid-fluid particle-assembled platforms. Laser irradiation causes the LSPR of plasmonic nanoparticles to generate intense electromagnetic fields localized on the surfaces of plasmonic nanoparticles, which in turn amplifies the Raman scattering signals of analyte molecules at the interface. SERS detection at fluid-fluid interfaces tackles the limitations of colorimetric, fluorescence, and electrochemical techniques by yielding rich molecular-level information of analytes, even at highly diluted concentration down to attomole levels.

Various 2D plasmonic arrays, including Au nanoparticles, Au nanorods, and Ag octahedra, have been employed to detect multiple analytes present in two segregated fluid phases. In particular, Au nanorod arrays have demonstrated polarization-dependent enhancement of SERS signals, with strongest SERS signals observed when the longitudinal LSPR mode of the nanorods are excited (Figure 9A).[26] These vertically-aligned Au nanorods at liquid-liquid interface achieve > 10^3-fold boost to SERS enhancement factor compared to randomly oriented rods.[108, 109] Indeed, the importance of crystal structure in achieving strong SERS signals is highlighted in the comparison of multiplex analyte detection using various Ag octahedra arrays of different crystal structures.[22] Square metacrystal arrays with plasmonic "hotstrips" gives rise to 10-fold signal enhancement as compared hexagonal close-packed arrays, with analytical enhancement factors reaching 10^8. These platforms clearly highlight the combined benefits of utilizing SERS detection at fluid-fluid interfaces to create a universal and ultrasensitive multiplex sensor. However, these 2D interfacial SERS platforms typically require large volume of liq-

uid(s) for their preparation, and are also susceptible to signal fluctuations due to inevitable thermal and physical agitations from the surroundings.

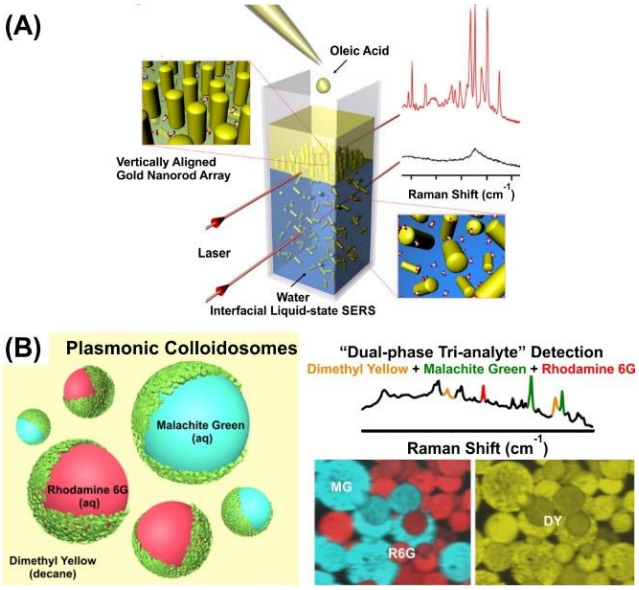

Figure 9. (A) Concurrent SERS sensing of analytes in aqueous and organic phases when laser is focused at the particle array assembled at the liquid-liquid interface. Reprinted with permission from ref 26. Copyright 2013 Nature Publishing Group. (B) Exploiting the picoliter-sized plasmonic colloidosomes for high throughput sensing via a dual-phase tri-analyte SERS detection scheme (left). Experimental SERS spectrum and SERS image (right) recorded using such plasmonic colloidosome-based interfacial detection platforms. Reprinted with permission from ref 29. Copyright 2015 Wiley-VCH verlag GmbH & Co.

Hence, the use of more robust miniature 3D SERS platforms, including plasmonic liquid marbles[24] and plasmonic colloidosomes,[29] has been used to circumvent the above limitations. Built from the clustering of Ag nanocubes on 3D soft interfaces, the plasmonic shell thickness of our liquid marbles/colloidosomes comprise approximately 12 inter-stacked nanoparticle layers. Extensive plasmonic coupling between adjacent nanocubes in three Cartesian planes generates intense and homogeneous SERS activities throughout the plasmonic shells (> 10^8-fold Raman signal enhancement). Furthermore, the curved surfaces and extended z-dimensions of these platforms gives rise to excellent tolerance to laser misalignment; multiple focal planes along the liquid marbles/colloidosomes are readily available to ensure that the laser is always focused on the 3D SERS platform. Consequently, plasmonic liquid marbles can achieve ultratrace analyte quantification down to sub-femtomole level using < 3 μL sample volume. In comparison, the > 27-fold expansion of SERS-active area upon emulsification of even smaller sample volumes (0.5 μL) empowers plasmonic colloidosomes to pushing the detection limits down to atto-mole levels.[29] Notably, we establish plasmonic colloidosomes as the first "dual-phase tri-analyte" detection scheme by exploiting their micro-scale dimensions (Figure 9B).

In addition, plasmonic colloidosomes also attain efficient and high-throughput SERS capabilities, giving rise to homogeneous and reproducible SERS signals with < 10 % intensity deviations in hyperspectral imaging experiments. This advantage enables us to couple plasmonic colloidosomes with fluidic channels to realize online, contamination-free, and rapid sequencing of multi-analyte inputs at the molecular-level. This flow system offers continuous online detection of 20 samples in less than 5 min with excellent signal reproducibility with ~9 % intensity deviation, which are important for high throughput (bio)chemical screening. Moreover, plasmonic colloidosomes can effectively isolate analyte samples to prevent cross-sample and channel contamination. Raman signatures and intensities of individual analytes remain unchanged during the interchange of plasmonic colloidosomes which contain various probe molecules with concentrations spanning five orders of magnitude (10^{-7} to 10^{-2} M). We foresee that both 3D interfacial sensors based on plasmonic liquid marbles and colloidosomes can also be easily extended to a vast range of encapsulating particles and solvent combinations, realizing targeted applications involving environmental and food safety, forensic, biomedical analysis, etc. [110-113]

2.3 Reaction and its monitoring at the soft interfaces

Particle-assembled fluid-fluid interfaces are ideal platforms to promote biphasic reactions, bringing together immiscible precursors to the interface and initiates their chemical reactions. Biphasic reactions are impossible to achieve using a single aqueous or organic phase reaction medium, and have important applications such as synthesis of large-area and ultrathin plate-like structures.[114] Here, we will discuss recent progress in using particle-assembled soft interfaces to modulate reaction kinetics, followed by a brief review on the in-situ tracking of reaction events using reactor-sensor hybrid based on these soft interfaces.

Organizing metallic nanoparticles at the fluid-fluid interface creates an active soft "electrocatalyst" to boost electrochemical performance vital in many energy-related reactions, such as hydrogen evolution and oxygen reduction reactions.[115] These nanoparticle films can be electrically polarized with ease to execute redox catalysis. The Fermi level of the electrons in these films can be easily manipulated to achieve direct control over the rate and direction of electron transfer between the electrode and redox species.[27] Cyclic voltammetry studies show that self-assembled Au nanoparticles at 2D water-trifluorotoluene interface facilitate the electron transfer between the nanoparticle film and model redox species comprising ferrocene/ferrocenium (organic phase electron donor) and $[Fe(CN)_6]^{3-/4-}$ (aqueous phase electron acceptor, Figure 10A). This improved electron transfer results in a > 1.5-fold increase of electrochemical performance using particle-assembled soft interface compared to their absence.

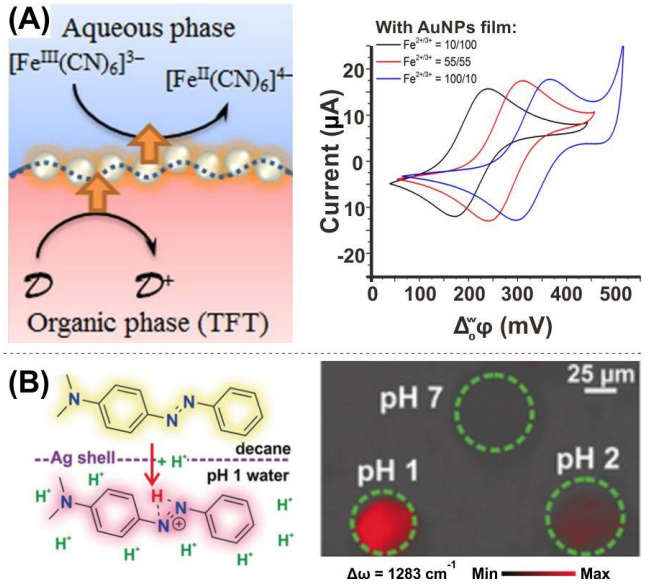

Figure 10. (A) Self-assembled Au nanoparticle film at the oil/water interface catalyzes an interfacial redox reaction. Reprinted with permission from ref 27. Copyright 2015 American Chemical Society. (B) Parallel control and tracking of reaction kinetics of liquid-liquid interfacial reactions. Molecular depiction (left) of the interfacial protonation of dimethyl yellow across the liquid-liquid interface using colloidosome encapsulated with aqueous acid. Parallel SERS imaging (right) of colloidosomes comprising of various pH values. Reprinted with permission from ref 23. Copyright 2016 Wiley-VCH verlag GmbH & Co.

In comparison to bulk 2D fluidic interface, the miniaturization of (bio)chemical processes in 3D droplet-based (liquid marbles and colloidosomes) reactors are advantageous for high throughput reaction screening and enhanced reaction kinetics. 3D droplet-based reactors reduce chemical/solvent consumption, possess increased surface area-to-volume ratio, and have shorter reactant diffusion paths in the milli/micrometric length scale. For instance, the degradation kinetics of methylene blue enclosed within catalytic liquid marble exhibits strong dependence on the size/volume of the microreactor.[75] Reducing the reaction droplet's volume from 80 to 5 μL enhances the degradation kinetics by 5-fold, attaining an optimal rate constant of 0.41 min^{-1} with an almost 100 % degradation efficiency in < 10 min. The appeal of liquid marbles and colloidosomes as miniature reactors is exemplified in their extensive applications in (bio)chemical reactions, including nanoparticle synthesis,[116] blood typing,[117] and even cell cultivation.[73]

In addition, microdroplet reaction kinetics can be easily enhanced by selecting encapsulating particles which can impart additional functionalities such as catalytic, photothermal and magnetic properties to the system. These properties can directly impact the rate and efficacy of intermolecular collisions between reactants, which form the basis of all bio(chemical) reactions. For example, silica beads-based liquid marbles are used to regulate silver mirror reactions.[82] Increasing the amount of deprotonated and negatively-charged silanol groups (Si-O-) on the beads promote their electrostatic interactions with positively-charged Ag ion, thus forming a silver ion layer bonded directly to the silica surface. Subsequent reduction of the Ag ions forms a Ag metal coating throughout the silica particles. This deposition method also offers a facile approach in the fabrication of Janus particles whereby Ag mirror can be selectively coated on half of the silica hemisphere that is exposed to the enclosed reacting solution.

Our group also employed the photothermal heating capabilities of graphene liquid marbles to linearly modulate the reaction kinetics of the enclosed microdroplets.[70] Graphene liquid marbles provide on-demand heating and cooling with temperature ramping rates reaching 1800 °C/s, enabling their surface temperatures to be regulated between 21 – 135 °C simply by irradiation of laser in the power range of 0 to 214 mW. Subsequent thermal conduction from the graphene shell to the encapsulated microdroplets allows the water droplet to attain maximum temperatures of 74 °C. This localized heating enables a linear kinetic modulation of dye degradation following Arrhenius equation, and enhances the degradation rate constant by > 12-fold as compared to room temperature kinetics. We foresee that such instantaneous photothermal heating will have tremendous prospects in on-demand activation of microreactions that are inert at room temperature, as well as for control over sequential process kinetics of multi-step reactions.

Magnetic field-responsive Fe_3O_4-based rotating liquid marbles present another attractive approach to boost reaction kinetics by directing reactants in the microdroplets to catalytically-active shells, thereby facilitating intermolecular and/or catalyst-reactant interactions.[72, 81] As its name implies, rotating liquid marbles rotate along their vertical axes in the presence of an external rotating magnetic field, and this rotation generates a spiral movement of encapsulated molecules towards the shell. This hydrodynamic flow is akin to the rotational behaviors in biological systems, enabling rapid molecular homogenization in the entire 3D microdroplet and accelerating mass advection towards the encapsulating shell. Rotation rates linearly modulate the shell-catalyzed degradation kinetics of malachite green, due to the directed transport of the dye molecules to the catalytic sites on the shell. As rotation rates increases from 0 to 1300 rpm, degradation kinetics improve by ~ 5-fold from 0.13 to 0.62 min^{-1}. In comparison to conventional stir bar-based convective flow which drives reactants towards the stir bar instead of the catalyst, the unique mass transfer mechanism in the rotating liquid marble enables a 3-fold faster acceleration of reactants toward a catalytically-active shell surface. Rotating liquid marbles are appealing magnetohydrodynamics transducer for control over mass transportation in microdroplet-based chemical, biological, and biomedical studies.

Achieving real-time assessment of chemical processes within the interfacial reactor is vital for the elucidation of reaction mechanism and dynamics, with the ultimate aim of optimizing reaction yield and selectivity through rational reaction design. Magnetic liquid marbles serve as a "lab in a droplet" system, where the magnetic shell can be opened/closed to monitor reaction progress using an external magnet.[33] Partial shell opening enables electrochemical-based identification of molecules using a miniaturized three-electrode probe, whereas fully opening the shell enables reaction species detection using transmission-based optical techniques such as UV-vis absorption. However, these ex-situ investigations are invasive, whereby reactions must be quenched/disrupted at predetermined stages for further elemental/molecular analysis.

In-situ reaction monitoring overcomes the limitations of ex-situ methods by tracking reaction events in their native environments without disturbing the reaction set-up. This approach enables a more representative identification and quantification of chemical species directly relevant to the reaction. Combin-

ing plasmonic liquid marbles and colloidosomes with SERS hyperspectral imaging creates an ideal platform for in-situ and time-resolved reaction tracking in their native environment through the particle shell. Molecular-specific vibrational fingerprints reflecting the chemical processes within a reaction microdroplet can be remotely tracked using such platforms.[25] Using diazonium-based moieties surface grafting as model reactions, we uncover a two-step sequential grafting process which begins with the initial Langmuir chemisorption of sulfonicbenzene diazonium onto Ag surface, followed by a 19-fold slower autocatalytic multilayer growth. Experimental findings corroborate well with theoretical simulations, allow us to elucidate the distinct process kinetics for the first time.

Plasmonic colloidosome-based microreactors are particularly ideal for unveiling interfacial processes owing to their large surface areas exposed to both dispersed and continuous phases, which also significantly shortens molecular diffusion lengths needed to access the entire 3D volume. Strong SERS enhancements from these plasmonic picoreactors further enable efficient tracking of interfacial molecular events. We demonstrate the on-site interfacial protonation of dimethyl yellow using this soft platform, and derive the reaction rate constant through SERS spectral evolution (Figure 10B).[23] Our ultrasensitive approach further allows differentiation of isomeric products, which cannot be distinguished using conventional analytical methods such as high performance liquid chromatography. By encapsulating aqueous solutions containing different chemical reagents, plasmonic colloidosomes are also attractive for high throughput monitoring and parallel control of multiple picoliter-scaled reactions. Our collective discussions highlight particle-assembled 2D and 3D soft interfaces as advanced reactor-sensor hybrids which are immensely beneficial for investigating small-volume reactions and/or interfacial phenomena prevalent in many (bio)chemical processes.

Conclusions

In this perspective, we have provided a brief overview on the recent progress of functional soft platforms formed via the assembly of particles at fluid-fluid interfaces. Current substrate-less platforms exist in various configurations, ranging from bulk 2D planar arrays trapped at phase boundaries to 3D microdroplet-based interfaces in the form of liquid marbles and colloidosomes. Both 2D and 3D interfacial platform formation are driven by the minimization of interfacial free energy, and we emphasize their unique physical/mechanical attributes which enable them to excel over conventional solid-based devices. We also provide an overview in applying these soft platforms to manipulate light-matter interactions, achieve multiplex molecular sensing, as well as modulate and elucidate reaction kinetics in microsystems. Their outstanding performance in these interfacial applications are superior over conventional solid substrate-based platforms.

In terms of future research, focus can be directed towards the creation of larger scale non-spherical soft interfaces. Geometric transformation of these 3D soft micro-interfaces can further enhance the surface area-to-volume ratios, with tremendous potential in boosting heterogeneous catalytic performance, interfacial reaction, surface-sensitive detection, and even uncovering unique photonics/magnetic phenomena. Current 3D soft interfaces are typically quasi-spherical, especially at the microscale. While non-spherical "armored bubbles" have been reported, these entities are formed individually via external physical forces such as compression, which is impractical for actual application.[118] Further work could also explore different techniques to form liquid marbles, with the aim of imparting collective properties that are unique to an ordered and ultrathin particle assembly at a macroscopic 3D fluid-fluid interface.

Another avenue of research could involve the facile preparation of multilayered droplet-based templates involving multiple fluid-fluid interfaces, such as oil-water-oil templates. These sophisticated designs are promising for the pre-programming of mass transfer within such hierarchical fluidic templates, enabling diffusion-controlled multi-step reaction and/or sequential reaction-purification automation. This unique platform-in-platform scheme can also induce multi-interfacial molecular phase transfers, possibly imparting "sieving" effect to sort targeted analytes from interfering species in multiplex detection of real and complex liquid matrices. Furthermore, such designs can also impart multiple functionalities to a single micro/pico-liter droplet that is highly symmetrical and uniform in all 3D space, in contrast to the current Janus-based configurations.

Finally, interfacial applications can be extended to other soft interfaces such as Leidenfrost droplets.[119, 120] Leidenfrost droplet is essentially a levitating liquid droplet produced via the formation of an underlying air cushion when the liquid is superheated on a hot surface. This superheated liquid droplet creates a unique internal Marangoni flow which can be utilized to enhance reactant homogenization and mixing. While particle assembly on Leidenfrost droplet has been demonstrated, there is no demonstration of the entire ensemble for interfacial applications. By combining Leidenfrost droplets with active encapsulating particles, we expect particle-assembled Leidenfrost droplets to provide a dynamic and non-equilibrium environment to kinetically-control (bio)chemical reactions and/or nanoparticle synthesis.[121, 122] Furthermore, research can also be directed to lengthen the lifetimes of these typically short-lived Leidenfrost droplets, which are shorter than 100 s. Longer Leidenfrost droplet lifetimes will also enable a more uniform chemical concentration within the droplets.[123]

All in all, given the collective benefits provided by particle-assembled soft interfaces, substrate-less platforms are clearly providing a paradigm shift to overcome the many limitations imposed by conventional solid-state devices. Through the boundless customizability and dynamic nature of interfacial particle assembly, we can certainly anticipate the continuous thriving of these platforms to realize a whole new level of exciting and diverse opportunities in various disciplines including nanotechnology, synthetic chemistry, photonics, and environmental and food safety.

AUTHOR INFORMATION

Corresponding Author

*X.Y.L. (xyling@ntu.edu.sg).

Author Contributions

[+]These authors contributed equally.

Notes

The authors declare no competing financial interest.

Biographies

Xing Yi Ling obtained her Ph.D. degree from University of Twente, the Netherlands in 2008. She did her post-doc research in Prof. Peidong Yang's group at the University of California, Berkeley with the Rubicon fellowship from the Netherlands Organization for Scientific Research. She joined NTU in 2011, and obtained her tenured associate professorship in 2016. She is the recipient of IUPAC Young Chemist award (2009), Singapore National Research Foundation fellowship (2012), the Asian and Oceanian Photochemistry Association prize for Young Scientist (2014), winner for L'ORÉAL Singapore for Women in Science National Fellowships (2015). Her research group focuses on the fabrication of surface-enhanced Raman scattering platforms by nanofabrication and/or self-assembly of shape-controlled noble metal nanocrystals for sensing and anti-counterfeiting applications.

Hiang Kwee Lee received his Bachelor's degree in Chemistry and Biological Chemistry from Nanyang Technological University (2013), Singapore. He is currently an A*STAR scholar and a Ph.D. candidate in nanomaterial chemistry at Nanyang Technological University, under the supervision of Prof. Xing Yi Ling and Dr. In Yee Phang. His research interests include the fabrication of substrate-less 2D and 3D functional platforms and their applications for toxin sensing, as well as reaction modulation and process monitoring.

Yih Hong Lee received his Ph.D. in Chemistry from National University of Singapore (2012). He is currently a research fellow under the guidance of Prof. Xing Yi Ling. His research interests include nanoparticle self-assembly, plasmonics, and optical behaviors of two-dimensional transition dichalcogenides. In nanoparticle self-assembly, he is interested in using nanoscale surface chemistry to direct the organization of nanoparticles into distinct metacrystals, and their applications as substrate-less sensing platforms.

Gia Chuong Phan-Quang received his Bachelor's degree in Chemistry and Biological Chemistry from Nanyang Technological University (2015), Singapore and continued to pursue a PhD degree in the same department. Chuong is currently researching on plasmonic micro-capsules, also known as plasmonic colloidosomes for detection and in-situ reaction screening at the picoliter scale.

Xuemei Han received her Bachelor's degree in Material Science and Engineering from Tianjin University (2007), China. In 2012, she received her PhD degree in Chemistry from the Technical Institute of Physics and Chemistry, University of Chinese Academy of Sciences, China. She served as an engineer at Beijing Institute of Opto-Electric Technology (2012-2014), China. She joined Prof. Xing Yi Ling's group as a research fellow at Nanyang Technological University, Singapore in 2014. Her current research interests focus on syntheses of plasmonic nanoparticles and their hybrid materials, fabrication of microreactor, in-situ reaction monitoring using SERS technique.

Charlynn Sher Lin Koh received her Bachelor's degree in Chemistry and Biological Chemistry from Nanyang Technological University (2016), Singapore. She was awarded the Nanyang President's Graduate Scholarship and is currently a pursuing her Ph.D. in nanomaterial chemistry at Nanyang Technological University. Her research interests include the use of substrate-less 2D and 3D platforms in multifunctional applications like in situ electrochemical-SERS, and integration of metal-organic frameworks in plasmonic nanoparticles.

ACKNOWLEDGMENT

X.Y.L. thanks the financial support from National Research Foundation, Singapore (NRF-NRFF2012-04), Singapore Ministry of Education, Tier 1 (RG21/16) and Tier 2 (MOE2016-T2-1-043) grants. H.K.L. appreciates the A*STAR Graduate Scholarship support from A*STAR, Singapore. G.C.P-Q and C.S.L.K acknowledge support from Nanyang Presidential Graduate Scholarship from Nanyang Technological University.

REFERENCES

1. Edel, J. B.; Kornyshev, A. A.; Kucernak, A. R.; Urbakh, M. Fundamentals and Applications of Self-Assembled Plasmonic Nanoparticles at Interfaces. *Chem. Soc. Rev.* **2016,** 45, *6*, 1581-1596.
2. Wu, J.; Ma, G.-H. Recent Studies of Pickering Emulsions: Particles Make the Difference. *Small* **2016,** 12, *34*, 4633-4648.
3. Aussillous, P.; Quéré, D. Liquid marbles. *Nature* **2001,** 411, *6840*, 924-927.
4. Dinsmore, A. D.; Hsu, M. F.; Nikolaides, M. G.; Marquez, M.; Bausch, A. R.; Weitz, D. A. Colloidosomes: Selectively Permeable Capsules Composed of Colloidal Particles. *Science* **2002,** 298, *5595*, 1006-1009.
5. Pieranski, P. Two-Dimensional Interfacial Colloidal Crystals. *Phys. Rev. Lett.* **1980,** 45, *7*, 569-572.
6. Binks, B. P.; Clint, J. H. Solid Wettability from Surface Energy Components: Relevance to Pickering Emulsions. *Langmuir* **2002,** 18, *4*, 1270-1273.
7. Aussillous, P.; Quéré, D. Properties of liquid marbles. *Proc. R. Soc. A* **2006,** 462, *2067*, 973-999.
8. Boker, A.; He, J.; Emrick, T.; Russell, T. P. Self-assembly of nanoparticles at interfaces. *Soft Matter* **2007,** 3, *10*, 1231-1248.
9. McHale, G.; Newton, M. I. Liquid marbles: topical context within soft matter and recent progress. *Soft Matter* **2015,** 11, *13*, 2530-2546.
10. Wong, T. S.; Kang, S. H.; Tang, S. K.; Smythe, E. J.; Hatton, B. D.; Grinthal, A.; Aizenberg, J. Bioinspired self-repairing slippery surfaces with pressure-stable omniphobicity. *Nature* **2011,** 477, *7365*, 443-7.
11. Ito, T.; Okazaki, S. Pushing the limits of lithography. *Nature* **2000,** 406, *6799*, 1027-1031.
12. Qin, D.; Xia, Y.; Whitesides, G. M. Soft lithography for micro- and nanoscale patterning. *Nat. Protoc.* **2010,** 5, *3*, 491-502.
13. Kim, P.; Kreder, M. J.; Alvarenga, J.; Aizenberg, J. Hierarchical or not? Effect of the length scale and hierarchy of the surface roughness on omniphobicity of lubricant-infused substrates. *Nano Lett.* **2013,** 13, *4*, 1793-9.
14. Hu, L. F.; Chen, M.; Fang, X. S.; Wu, L. M. Oil-Water Interfacial Self-Assembly: A Novel Strategy for Nanofilm and Nanodevice Fabrication. *Chem. Soc. Rev.* **2012,** 41, *3*, 1350-1362.
15. Li, W.; Yue, Q.; Deng, Y. H.; Zhao, D. Y. Ordered Mesoporous Materials Based on Interfacial Assembly and Engineering. *Adv. Mater.* **2013,** 25, 5129-5152.
16. McHale, G.; Newton, M. I. Liquid marbles: principles and applications. *Soft Matter* **2011,** 7, *12*, 5473-5481.
17. Bormashenko, E. New insights into liquid marbles. *Soft Matter* **2012,** 8, *43*, 11018-11021.
18. Bormashenko, E. Liquid marbles: Properties and applications. *Curr. Opin. Colloid Interface Sci.* **2011,** 16, *4*, 266-271.
19. Singh, G.; Chan, H.; Baskin, A.; Gelman, E.; Repnin, N.; Kral, P.; Klajn, R. Self-Assembly of Magnetite Nanocubes into Helical Superstructures. *Science* **2014,** 345, *6201*, 1149-1153.
20. Liu, D.; Zhou, F.; Li, C.; Zhang, T.; Zhang, H.; Cai, W.; Li, Y. Black Gold: Plasmonic Colloidosomes with Broadband Absorption Self-Assembled from Monodispersed Gold

Nanospheres by Using a Reverse Emulsion System. *Angew. Chem. Int. Ed.* **2015,** 54, *33*, 9596-9600.

21. Wang, D.; Zhu, L.; Chen, J.-F.; Dai, L. Liquid Marbles Based on Magnetic Upconversion Nanoparticles as Magnetically and Optically Responsive Miniature Reactors for Photocatalysis and Photodynamic Therapy. *Angew. Chem. Int. Ed.* **2016,** 55, *36*, 10795-10799.

22. Lee, Y. H.; Shi, W.; Lee, H. K.; Jiang, R.; Phang, I. Y.; Cui, Y.; Isa, L.; Yang, Y.; Wang, J.; Li, S.; Ling, X. Y. Nanoscale Surface Chemistry Directs the Tunable Assembly of Silver Octahedra into Three Two-Dimensional Plasmonic Superlattices. *Nat. Commun.* **2015,** 6, 6990.

23. Phan-Quang, G. C.; Lee, H. K.; Ling, X. Y. Isolating Reactions at the Picoliter Scale: Parallel Control of Reaction Kinetics at the Liquid–Liquid Interface. *Angew. Chem. Int. Ed.* **2016,** 55, *29*, 8304-8308.

24. Lee, H. K.; Lee, Y. H.; Phang, I. Y.; Wei, J.; Miao, Y. E.; Liu, T.; Ling, X. Y. Plasmonic liquid marbles: a miniature substrate-less SERS platform for quantitative and multiplex ultratrace molecular detection. *Angew. Chem. Int. Ed.* **2014,** 53, *20*, 5054-5058.

25. Han, X.; Lee, H. K.; Lee, Y. H.; Hao, W.; Liu, Y.; Phang, I. Y.; Li, S.; Ling, X. Y. Identifying Enclosed Chemical Reaction and Dynamics at the Molecular Level Using Shell-Isolated Miniaturized Plasmonic Liquid Marble. *J. Phys. Chem. Lett.* **2016,** 7, *8*, 1501-1506.

26. Kim, K.; Han, H. S.; Choi, I.; Lee, C.; Hong, S.; Suh, S.-H.; Lee, L. P.; Kang, T. Interfacial liquid-state surface-enhanced Raman spectroscopy. *Nat. Commun.* **2013,** 4, 2182.

27. Smirnov, E.; Peljo, P.; Scanlon, M. D.; Girault, H. H. Interfacial Redox Catalysis on Gold Nanofilms at Soft Interfaces. *ACS Nano* **2015,** 9, *6*, 6565-6575.

28. Ma, Y.; Liu, H.; Mao, M.; Meng, J.; Yang, L.; Liu, J. Surface-Enhanced Raman Spectroscopy on Liquid Interfacial Nanoparticle Arrays for Multiplex Detecting Drugs in Urine. *Anal. Chem.* **2016,** 88, *16*, 8145-8151.

29. Phan-Quang, G. C.; Lee, H. K.; Phang, I. Y.; Ling, X. Y. Plasmonic Colloidosomes as Three-Dimensional SERS Platforms with Enhanced Surface Area for Multiphase Sub-Microliter Toxin Sensing. *Angew. Chem. Int. Ed.* **2015,** 54, *33*, 9691-9695.

30. Hsu, M. F.; Nikolaides, M. G.; Dinsmore, A. D.; Bausch, A. R.; Gordon, V. D.; Chen, X.; Hutchinson, J. W.; Weitz, D. A.; Marquez, M. Self-assembled Shells Composed of Colloidal Particles: Fabrication and Characterization. *Langmuir* **2005,** 21, *7*, 2963-2970.

31. Thompson, K. L.; Williams, M.; Armes, S. P. Colloidosomes: Synthesis, properties and applications. *J. Colloid Interface Sci.* **2015,** 447, 217-228.

32. Phan-Quang, G. C.; Wee, E. H. Z.; Yang, F.; Lee, H. K.; Phang, I. Y.; Feng, X.; Alvarez-Puebla, R. A.; Ling, X. Y. Online Flowing Colloidosomes for Sequential Multi-analyte High-Throughput SERS Analysis. *Angew. Chem. Int. Ed.* **2017,** 56, *20*, 5565-5569.

33. Zhao, Y.; Xu, Z.; Niu, H.; Wang, X.; Lin, T. Magnetic liquid marbles: toward "Lab in a Droplet". *Adv. Funct. Mater.* **2015,** 25, *3*, 437-444.

34. De Angelis, F.; Gentile. F; Mecarini. F; Das. G; Moretti. M; Candeloro. P; Coluccio, M. L.; Cojoc. G; Accardo. A; Liberale. C; Zaccaria, R. P.; Perozziello. G; Tirinato. L; Toma. A; Cuda. G; Cingolani. R; Di Fabrizio, E. Breaking the diffusion limit with super-hydrophobic delivery of molecules to plasmonic nanofocusing SERS structures. *Nat. Photon.* **2011,** 5, *11*, 682-687.

35. Li, X.; Lee, H. K.; Phang, I. Y.; Lee, C. K.; Ling, X. Y. Superhydrophobic-Oleophobic Ag Nanowire Platform: An Analyte-Concentrating and Quantitative Aqueous and Organic Toxin Surface-Enhanced Raman Scattering Sensor. *Anal. Chem.* **2014,** 86, *20*, 10437-10444.

36. Zhang, Q.; Lee, Y. H.; Phang, I. Y.; Lee, C. K.; Ling, X. Y. Hierarchical 3D SERS Substrates Fabricated by Integrating Photolithographic Microstructures and Self-Assembly of Silver Nanoparticles. *Small* **2014,** 10, *13*, 2703-2711.

37. Whitesides, G. M. The origins and the future of microfluidics. *Nature* **2006,** 442, *7101*, 368-373.

38. deMello, A. J. Control and detection of chemical reactions in microfluidic systems. *Nature* **2006,** 442, *7101*, 394-402.

39. El-Ali, J.; Sorger, P. K.; Jensen, K. F. Cells on chips. *Nature* **2006,** 442, *7101*, 403-411.

40. Janasek, D.; Franzke, J.; Manz, A. Scaling and the design of miniaturized chemical-analysis systems. *Nature* **2006,** 442, *7101*, 374-380.

41. van der Stam, W.; Gantapara, A. P.; Akkerman, Q. A.; Soligno, G.; Meeldijk, J. D.; van Roij, R.; Dijkstra, M.; Donega, C. d. M. Self-Assembly of Colloidal Hexagonal Bipyramid- and Bifrustum-Shaped ZnS Nanocrystals into Two-Dimensional Superstructures. *Nano lett.* **2014,** 14, *2*, 1032-1037.

42. Yang, Y. J.; Lee, Y. H.; Phang, I. Y.; Jiang, R. B.; Sim, H. Y. F.; Wang, J. F.; Ling, X. Y. A Chemical Approach To Break the Planar Configuration of Ag Nanocubes into Tunable Two-Dimensional Metasurfaces. *Nano lett.* **2016,** 16, 3872-3878.

43. Cavallaro, M., Jr.; Botto, L.; Lewandowski, E. P.; Wang, M.; Stebe, K. J. Curvature-Driven Capillary Migration and Assembly of Rod-Like Particles. *Proc. Natl. Acad. Sci.* **2011,** 108, *52*, 20923-20928.

44. Botto, L.; Lewandowski, E. P.; Cavallaro, M., Jr.; Stebe, K. J. Capillary interactions between anisotropic particles. *Soft Matter* **2012,** 8, *39*, 9957-9971.

45. Srivastava, S.; Nykypanchuk, D.; Fukuto, M.; Gang, O. Tunable Nanoparticle Arrays at Charged Interfaces. *ACS Nano* **2014,** 8, *10*, 9857-9866.

46. von Freymann, G.; Kitaev, V.; Lotschz, B. V.; Ozin, G. A. Bottom-Up Assembly of Photonic Crystals. *Chem. Soc. Rev.* **2013,** 42, 2528-2554.

47. Zhang, S. Y.; Regulacio, M. D.; Han, M. Y. Self-Assembly of Colloidal One-Dimensional Nanocrystals. *Chem. Soc. Rev.* **2014,** 43, 2301-2323.

48. Booth, S. G.; Dryfe, R. A. W. Assembly of Nanoscale Objects at the Liquid/Liquid Interface. *J. Phys. Chem. C* **2015,** 119, 23295-23309.

49. Matharu, Z.; Bandodkar, A. J.; Gupta, V.; Malhotra, B. D. Fundamentals and application of ordered molecular assemblies to affinity biosensing. *Chem. Soc. Rev.* **2012,** 41, *3*, 1363-1402.

50. Tao, A. R.; Huang, J. X.; Yang, P. D. Langmuir-Blodgettry of Nanocrystals and Nanowires. *Acc. Chem. Res.* **2008,** 41, 1662-1673.

51. Lee, H. K.; Lee, Y. H.; Zhang, Q.; Phang, I. Y.; Tan, J. M. R.; Cui, Y.; Ling, X. Y. Superhydrophobic Surface-Enhanced Raman Scattering Platform Fabricated by Assembly of Ag Nanocubes for Trace Molecular Sensing. *ACS Appl. Mater. Inter.* **2013,** 5, *21*, 11409-11418.

52. Lau, C. Y.; Duan, H. G.; Wang, F. K.; He, C. B.; Low, H. Y.; Yang, J. K. W. Enhanced Ordering in Gold Nanoparticles Self-Assembly through Excess Free Ligands. *Langmuir* **2011,** 27, 3355-3360.

53. Wen, T. L.; Majetich, S. A. Ultra-Large-Area Self-Assembled Mono layers of Nanoparticles. *ACS Nano* **2011,** 5, 8868-8876.

54. Lee, Y. H.; Lee, C. K.; Tan, B.; Tan, J. M. R.; Phang, I. Y.; Ling, X. Y. Using the Langmuir-Schaefer Technique to Fabricate Large-Area Dense SERS-Active Au Nanoprism Monolayer Films. *Nanoscale* **2013,** 5, 6404-6412.

55. Alvarez-Puebla, R. A.; Agarwal, A.; Manna, P.; Khanal, B. P.; Aldeanueva-Potel, P.; Carbo-Argibay, E.; Pazos-Perez, N.; Vigderman, L.; Zubarev, E. R.; Kotov, N. A.; Liz-Marzan, L. M. Gold nanorods 3D-supercrystals as surface enhanced Raman

scattering spectroscopy substrates for the rapid detection of scrambled prions. *Proc. Natl. Acad. Sci. U. S. A.* **2011,** 108, *20*, 8157-61.

56. Pietra, F.; Rabouw, F. T.; Evers, W. H.; Byelov, D. V.; Petukhov, A. V.; Donega, C. D.; Vanmaekelbergh, D. Semiconductor Nanorod Self-Assembly at the Liquid/Air Interface Studied by in Situ GISAXS and ex Situ TEM. *Nano lett.* **2012,** 12, *11*, 5515-5523.

57. Dong, A.; Chen, J.; Vora, P. M.; Kikkawa, J. M.; Murray, C. B. Binary Nanocrystal Superlattice Membranes Self-Assembled at the Liquid-Air Interface. *Nature* **2010,** 466, *7305*, 474-477.

58. Chen, J.; Dong, A.; Cai, J.; Ye, X.; Kang, Y.; Kikkawa, J. M.; Murray, C. B. Collective Dipolar Interactions in Self-Assembled Magnetic Binary Nanocrystal Superlattice Membranes. *Nano lett.* **2010,** 10, *12*, 5103-5108.

59. Dong, A. G.; Ye, X. C.; Chen, J.; Murray, C. B. Two-Dimensional Binary and Ternary Nanocrystal Superlattices: The Case of Monolayers and Bilayers. *Nano lett.* **2011,** 11, *4*, 1804-1809.

60. Paik, T.; Diroll, B. T.; Kagan, C. R.; Murray, C. B. Binary and Ternary Superlattices Self-Assembled from Colloidal Nanodisks and Nanorods. *J. Am. Chem. Soc.* **2015,** 137, *20*, 6662-6669.

61. Ye, X.; Chen, J.; Engel, M.; Millan, J. A.; Li, W.; Qi, L.; Xing, G.; Collins, J. E.; Kagan, C. R.; Li, J.; Glotzer, S. C.; Murray, C. B. Competition of Shape and Interaction Patchiness for Self-Assembling Nanoplates. *Nat. Chem.* **2013,** 5, *6*, 466-473.

62. Nie, H. L.; Dou, X.; Tang, Z. H.; Jang, H. D.; Huang, J. X. High-Yield Spreading of Water-Miscible Solvents on Water for Langmuir-Blodgett Assembly. *J. Am. Chem. Soc.* **2015,** 137, *33*, 10683-10688.

63. Park, Y. K.; Park, S. Directing Close-Packing of Midnanosized Gold Nanoparticles at A Water/Hexane Interface. *Chem. Mater.* **2008,** 20, *6*, 2388-2393.

64. Isa, L.; Kumar, K.; Mueller, M.; Grolig, J.; Textor, M.; Reimhult, E. Particle Lithography from Colloidal Self-Assembly at Liquid-Liquid Interfaces. *ACS Nano* **2010,** 4, *10*, 5665-5670.

65. Armao Iv, J. J.; Nyrkova, I.; Fuks, G.; Osypenko, A.; Maaloum, M.; Moulin, E.; Arenal, R.; Gavat, O.; Semenov, A.; Giuseppone, N. Anisotropic Self-Assembly of Supramolecular Polymers and Plasmonic Nanoparticles at the Liquid-Liquid Interface. *J. Am. Chem. Soc.* **2017,** 139, *6*, 2345-2350.

66. Bormashenko, E.; Balter, S.; Bormashenko, Y.; Aurbach, D. Honeycomb structures obtained with breath figures self-assembly allow water/oil separation. *Colloids Surf., A* **2012,** 415, 394-398.

67. Boker, A.; Lin, Y.; Chiapperini, K.; Horowitz, R.; Thompson, M.; Carreon, V.; Xu, T.; Abetz, C.; Skaff, H.; Dinsmore, A. D.; Emrick, T.; Russell, T. P. Hierarchical nanoparticle assemblies formed by decorating breath figures. *Nat. Mater.* **2004,** 3, *5*, 302-6.

68. Xue, Y.; Wang, H.; Zhao, Y.; Dai, L.; Feng, L.; Wang, X.; Lin, T. Magnetic Liquid Marbles: A "Precise" Miniature Reactor. *Adv. Mater.* **2010,** 22, *43*, 4814-4818.

69. Dandan, M.; Erbil, H. Y. Evaporation rate of graphite liquid marbles: comparison with water droplets. *Langmuir* **2009,** 25, *14*, 8362-8367.

70. Gao, W.; Lee, H. K.; Hobley, J.; Liu, T.; Phang, I. Y.; Ling, X. Y. Graphene liquid marbles as photothermal miniature reactors for reaction kinetics modulation. *Angew. Chem. Int. Ed.* **2015,** 54, *13*, 3993-3996.

71. Sivan, V.; Tang, S. Y.; O'Mullane, A. P.; Petersen, P.; Eshtiaghi, N.; Kalantar-zadeh, K.; Mitchell, A. Liquid metal marbles. *Adv. Funct. Mater.* **2013,** 23, *2*, 144-152.

72. Han, X.; Lee, H. K.; Lim, W. C.; Lee, Y. H.; Phan-Quang, G. C.; Phang, I. Y.; Ling, X. Y. Spinning liquid marble and its dual applications as microcentrifuge and miniature localized viscometer. *ACS Appl. Mater. & Interfaces* **2016,** 8, *36*, 23941-23946.

73. Vadivelu, R. K.; Ooi, C. H.; Yao, R. Q.; Tello Velasquez, J.; Pastrana, E.; Diaz-Nido, J.; Lim, F.; Ekberg, J. A.; Nguyen, N. T.; St John, J. A. Generation of three-dimensional multiple spheroid model of olfactory ensheathing cells using floating liquid marbles. *Sci. Rep.* **2015,** 5, 15083.

74. Bormashenko, E.; Pogreb, R.; Musin, A. Stable water and glycerol marbles immersed in organic liquids: from liquid marbles to Pickering-like emulsions. *J. Colloid Interface Sci.* **2012,** 366, *1*, 196-9.

75. Miao, Y.-E.; Lee, H. K.; Chew, W. S.; Phang, I. Y.; Liu, T.; Ling, X. Y. Catalytic liquid marbles: Ag nanowire-based miniature reactors for highly efficient degradation of methylene blue. *Chem. Commun.* **2014,** 50, *44*, 5923-5926.

76. Paven, M.; Mayama, H.; Sekido, T.; Butt, H. J.; Nakamura, Y.; Fujii, S. Light-driven delivery and release of materials using liquid marbles. *Adv. Funct. Mater.* **2016,** 26, *19*, 3199-3206.

77. Liu, Z.; Fu, X.; Binks, B. P.; Shum, H. C. Coalescence of electrically charged liquid marbles. *Soft Matter* **2016,** 13, 119-124.

78. Zhao, Y.; Fang, J.; Wang, H.; Wang, X.; Lin, T. Magnetic liquid marbles: manipulation of liquid droplets using highly hydrophobic Fe3O4 nanoparticles. *Adv. Mater.* **2010,** 22, *6*, 707-710.

79. Kavokine, N.; Anyfantakis, M.; Morel, M.; Rudiuk, S.; Bickel, T.; Baigl, D. Light-driven transport of a liquid marble with and against surface flows. *Angew. Chem. Int. Ed.* **2016,** 55, 11183-11187.

80. Bormashenko, E.; Bormashenko, Y.; Grynyov, R.; Aharoni, H.; Whyman, G.; Binks, B. P. Self-Propulsion of Liquid Marbles: Leidenfrost-like Levitation Driven by Marangoni Flow. *J. Phys. Chem. C* **2015,** 119, *18*, 9910-9915.

81. Han, X.; Lee, H. K.; Lee, Y. H.; Ling, X. Y. Dynamic Rotating Liquid Marble for Directional and Enhanced Mass Transportation in Three-Dimensional Microliter Droplets. *J. Phys. Chem. Lett.* **2017,** 8, *1*, 243-249.

82. Sheng, Y.; Sun, G.; Wu, J.; Ma, G.; Ngai, T. Silica-based liquid marbles as microreactors for the silver mirror reaction. *Angew. Chem. Int. Ed.* **2015,** 127, *24*, 7118-7123.

83. Bibette, J.; Leal-Calderon, F.; Schmitt, V.; Poulin, P., *Emulsion Science: Basic Principles. An Overview*. Springer Berlin Heidelberg: 2003.

84. Vázquez-Vázquez, C.; Vaz, B.; Giannini, V.; Pérez-Lorenzo, M.; Alvarez-Puebla, R. A.; Correa-Duarte, M. A. Nanoreactors for Simultaneous Remote Thermal Activation and Optical Monitoring of Chemical Reactions. *J. Am. Chem. Soc.* **2013,** 135, *37*, 13616-13619.

85. Kurayama, F.; Yoshikawa, T.; Furusawa, T.; Bahadur, N. M.; Handa, H.; Sato, M.; Suzuki, N. Microcapsule with a heterogeneous catalyst for the methanolysis of rapeseed oil. *Bioresour. Technol.* **2013,** 135, 652-658.

86. Samanta, B.; Yang, X.-C.; Ofir, Y.; Park, M.-H.; Patra, D.; Agasti, S. S.; Miranda, O. R.; Mo, Z.-H.; Rotello, V. M. Catalytic Microcapsules Assembled from Enzyme–Nanoparticle Conjugates at Oil–Water Interfaces. *Angew. Chem. Int. Ed.* **2009,** 48, *29*, 5341-5344.

87. Sanles-Sobrido, M.; Exner, W.; Rodríguez-Lorenzo, L.; Rodríguez-González, B.; Correa-Duarte, M. A.; Álvarez-Puebla, R. A.; Liz-Marzán, L. M. Design of SERS-Encoded, Submicron, Hollow Particles Through Confined Growth of Encapsulated Metal Nanoparticles. *J. Am. Chem. Soc.* **2009,** 131, *7*, 2699-2705.

88. Piradashvili, K.; Alexandrino, E. M.; Wurm, F. R.; Landfester, K. Reactions and Polymerizations at the Liquid–Liquid Interface. *Chem. Rev*, **2016,** 116, *4*, 2141-2169.

89. De Geest, B. G.; Van Camp, W.; Du Prez, F. E.; De Smedt, S. C.; Demeester, J.; Hennink, W. E. Biodegradable

microcapsules designed via 'click' chemistry. *Chem. Commun.* **2008**, *2*, 190-192.

90. Sahu, P.; Ali, S. M.; Shenoy, K. T. Test of Universal Scaling Law for Molecular Diffusion of Liquids in Bulk and Nanotube Confinement. *J. Phys. Chem. C* **2017**.

91. Li, M.; Harbron, R. L.; Weaver, J. V.; Binks, B. P.; Mann, S. Electrostatically gated membrane permeability in inorganic protocells. *Nat. Chem.* **2013,** 5, *6*, 529-36.

92. Giner-Casares, J. J.; Liz-Marzan, L. M. Plasmonic Nanoparticles in 2D for Biological Applications: Toward Active Multipurpose Platforms. *Nano Today* **2014,** 9, *3*, 365-377.

93. Gómez-Graña, S.; Pérez-Juste, J.; Alvarez-Puebla, R. A.; Guerrero-Martínez, A.; Liz-Marzán, L. M. Self-Assembly of Au@Ag Nanorods Mediated by Gemini Surfactants for Highly Efficient SERS-Active Supercrystals. *Adv. Opt. Mater.* **2013,** 1, *7*, 477-481.

94. Abalde-Cela, S.; Auguie, B.; Fischlechner, M.; Huck, W. T. S.; Alvarez-Puebla, R. A.; Liz-Marzan, L. M.; Abell, C. Microdroplet fabrication of silver-agarose nanocomposite beads for SERS optical accumulation. *Soft Matter* **2011,** 7, *4*, 1321-1325.

95. Zhang, S. Z.; Sun, L. D.; Tian, H.; Liu, Y.; Wang, J. F.; Yan, C. H. Reversible luminescence switching of NaYF4:Yb,Er nanoparticles with controlled assembly of gold nanoparticles. *Chem. Commun.* **2009**, *18*, 2547-9.

96. Kang, Y. J.; Ye, X. C.; Chen, J.; Cai, Y.; Diaz, R. E.; Adzic, R. R.; Stach, E. A.; Murray, C. B. Design of Pt-Pd Binary Superlattices Exploiting Shape Effects and Synergistic Effects for Oxygen Reduction Reactions. *J. Am. Chem. Soc.* **2013,** 135, *1*, 42-45.

97. Wang, Z. H.; Liu, Y. M.; Tao, P.; Shen, Q. C.; Yi, N.; Zhang, F. Y.; Liu, Q. L.; Song, C. Y.; Zhang, D.; Shang, W.; Deng, T. Bio-Inspired Evaporation Through Plasmonic Film of Nanoparticles at the Air-Water Interface. *Small* **2014,** 10, *16*, 3234-3239.

98. Yang, Z. L.; Chen, S.; Fang, P. P.; Ren, B.; Girault, H. H.; Tian, Z. Q. LSPR Properties of Metal Nanoparticles Adsorbed at a Liquid-Liquid Interface. *Phys. Chem. Chem. Phys.* **2013,** 15, *15*, 5374-5378.

99. Tao, A.; Sinsermsuksakul, P.; Yang, P. Tunable plasmonic lattices of silver nanocrystals. *Nat. Nanotechnol.* **2007,** 2, *7*, 435-40.

100. Yen, Y. T.; Lu, T. Y.; Lee, Y. C.; Yu, C. C.; Tsai, Y. C.; Tseng, Y. C.; Chen, H. L. Highly Reflective Liquid Mirrors: Exploring the Effects of Localized Surface Plasmon Resonance and the Arrangement of Nanoparticles on Metal Liquid-like Films. *ACS Appl. Mater. Inter.* **2014,** 6, *6*, 4292-4300.

101. Smirnov, E.; Peljo, P.; Scanlon, M. D.; Gumy, F.; Girault, H. H. Self-Healing Gold Mirrors and Filters at Liquid-Liquid Interfaces. *Nanoscale* **2016,** 8, *14*, 7723-7737.

102. Fang, P. P.; Chen, S.; Deng, H. Q.; Scanlon, M. D.; Gumy, F.; Lee, H. J.; Momotenko, D.; Amstutz, V.; Cortes-Salazar, F.; Pereira, C. M.; Yang, Z. L.; Girault, H. H. Conductive Gold Nanoparticle Mirrors at Liquid/Liquid Interfaces. *ACS Nano* **2013,** 7, *10*, 9241-9248.

103. Collier, C. P.; Saykally, R. J.; Shiang, J. J.; Henrichs, S. E.; Heath, J. R. Reversible Tuning of Silver Quantum Dot Monolayers Through the Metal-Insulator Transition. *Science* **1997,** 277, *5334*, 1978-1981.

104. Turek, V. A.; Cecchini, M. P.; Paget, J.; Kucernak, A. R.; Kornyshev, A. A.; Edel, J. B. Plasmonic Ruler at the Liquid-Liquid Interface. *ACS Nano* **2012,** 6, *9*, 7789-7799.

105. Tian, J.; Arbatan, T.; Li, X.; Shen, W. Liquid marble for gas sensing. *Chem. Commun.* **2010,** 46, *26*, 4734-4736.

106. Kim, H. R.; Pereira, C. M.; Han, H. Y.; Lee, H. J. Voltammetric Studies of Topotecan Transfer Across Liquid/Liquid Interfaces and Sensing Applications. *Anal. Chem.* **2015,** 87, *10*, 5356-5362.

107. Shen, X.; Xu, C.; Uddin, K. M. A.; Larsson, P.-O.; Ye, L. Molecular recognition with colloidosomes enabled by imprinted polymer nanoparticles and fluorogenic boronic acid. *J. Mater. Chem. B* **2013,** 1, *36*, 4612-4618.

108. Cui, Y.; Hegde, R. S.; Phang, I. Y.; Lee, H. K.; Ling, X. Y. Encoding molecular information in plasmonic nanostructures for anti-counterfeiting applications. *Nanoscale* **2014,** 6, *1*, 282-288.

109. Cui, Y.; Phang, I. Y.; Hegde, R. S.; Lee, Y. H.; Ling, X. Y. Plasmonic Silver Nanowire Structures for Two-Dimensional Multiple-Digit Molecular Data Storage Application. *ACS Photonics* **2014,** 1, *7*, 631-637.

110. Colombo, M.; Fiandra, L.; Alessio, G.; Mazzucchelli, S.; Nebuloni, M.; De Palma, C.; Kantner, K.; Pelaz, B.; Rotem, R.; Corsi, F.; Parak, W. J.; Prosperi, D. Tumour homing and therapeutic effect of colloidal nanoparticles depend on the number of attached antibodies. *Nat. Commun.* **2016,** 7, 13818.

111. Caruso, F.; Caruso, R. A.; Möhwald, H. Nanoengineering of Inorganic and Hybrid Hollow Spheres by Colloidal Templating. *Science* **1998,** 282, *5391*, 1111-1114.

112. Cayre, O. J.; Hitchcock, J.; Manga, M. S.; Fincham, S.; Simoes, A.; Williams, R. A.; Biggs, S. pH-responsive colloidosomes and their use for controlling release. *Soft Matter* **2012,** 8, *17*, 4717-4724.

113. Yow, H. N.; Routh, A. F. Formation of liquid core-polymer shell microcapsules. *Soft Matter* **2006,** 2, *11*, 940-949.

114. Ameloot, R.; Vermoortele, F.; Vanhove, W.; Roeffaers, M. B.; Sels, B. F.; De Vos, D. E. Interfacial synthesis of hollow metal-organic framework capsules demonstrating selective permeability. *Nat. Chem.* **2011,** 3, *5*, 382-7.

115. Smirnov, E.; Peljo, P.; Scanlon, M. D.; Girault, H. H. Gold Nanofilm Redox Catalysis for Oxygen Reduction at Soft Interfaces. *Electrochim. Acta* **2016,** 197, 362-373.

116. Chu, Y.; Wang, Z.; Pan, Q. Constructing robust liquid marbles for miniaturized synthesis of graphene/Ag nanocomposite. *ACS Appl. Mater. Interfaces* **2014,** 6, *11*, 8378-86.

117. Arbatan, T.; Li, L.; Tian, J.; Shen, W. Liquid Marbles as Micro-bioreactors for Rapid Blood Typing. *Adv. Healthcare Mater.* **2012,** 1, *1*, 80-83.

118. Bala Subramaniam, A.; Abkarian, M.; Mahadevan, L.; Stone, H. A. Colloid science: Non-spherical bubbles. *Nature* **2005,** 438, *7070*, 930-930.

119. Lagubeau, G.; Le Merrer, M.; Clanet, C.; Quere, D. Leidenfrost on a ratchet. *Nature Phys.* **2011,** 7, *5*, 395-398.

120. Hao, C.; Liu, Y.; Chen, X.; Li, J.; Zhang, M.; Zhao, Y.; Wang, Z. Bioinspired Interfacial Materials with Enhanced Drop Mobility: From Fundamentals to Multifunctional Applications. *Small* **2016,** 12, *14*, 1825-1839.

121. Abdelaziz, R.; Disci-Zayed, D.; Hedayati, M. K.; Pöhls, J.-H.; Zillohu, A. U.; Erkartal, B.; Chakravadhanula, V. S. K.; Duppel, V.; Kienle, L.; Elbahri, M. Green chemistry and nanofabrication in a levitated Leidenfrost drop. *Nat. Commun.* **2013,** 4, 2400.

122. Lim, C. H.; Kang, H.; Kim, S.-H. Colloidal Assembly in Leidenfrost Drops for Noniridescent Structural Color Pigments. *Langmuir* **2014,** 30, *28*, 8350-8356.

123. Biance, A.-L.; Clanet, C.; Quéré, D. Leidenfrost drops. *Phys. Fluids* **2003,** 15, *6*, 1632-1637.

Table of Contents (TOC)